Action potential generation in small cell lung cancer cells

Jodie Collingridge and Hugh P.C. Robinson

Department of Physiology, Development, and Neuroscience, University of Cambridge, Cambridge, United Kingdom

Introduction: intrinsic electrical activity drives small-cell lung cancer (SCLC) progression

SCLC is an aggressive form of neuroendocrine (NE) cancer characterised by poor prognosis and a high rate of metastasis[1]. NE cancers exhibit many of the molecular characteristics of neuronal cells, including upregulated expression of voltage-gated ion channels and membrane excitability. Recently, we demonstrated that the electrical activity of NE cancers such as SCLC directly drives tumour progression[2]. Given their apparent role in disease progression, ion channels may present an emerging target for the treatment and further understanding of challenging NE cancers such as SCLC.

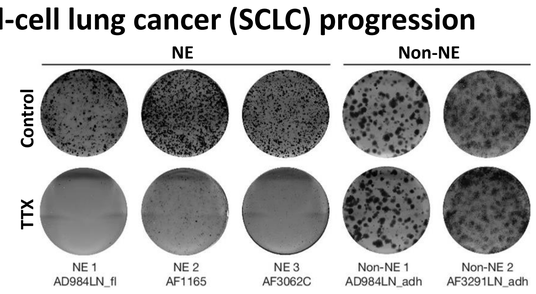

Figure 1. TTX blocks colony formation of excitable NE, but not non-NE, cancer cells (Peinado *et. al.*, 2025).

AIMS

- Characterise electrophysiology of SCLC lines and identify functional ion channel populations.
- Explore selected ion channels as targets for modulating the excitability of SCLC cells.
- Refine a mathematical model for simulating SCLC cell excitability.
- Explore the impact of modulating excitability on SCLC cell function, proliferation, and metastasis.

Methods

Whole-cell patch-clamp electrophysiology was performed on the human SCLC cell line NCI-H889[3] and AF1165 cells derived from a SCLC mouse model primary tumour[4,5]. Experiments were performed as previously described[2]. Statistical analyses were performed in MATLAB[6]. For voltage-clamp data, leak subtraction was performed as $I_{leak}=G_{leak}(V-E_{leak})$. Boltzman curves were fit as $G/G_{max}=1/(1+\exp((V_{1/2}-V)/k))$. Statistical tests are one way ANOVA with Dunn-Šidák post-hoc correction unless otherwise stated, *p<0.05, **p<0.01, ***p<0.001, ****p<0.0001.

Voltage- and current-clamp step protocols are as below unless otherwise specified:

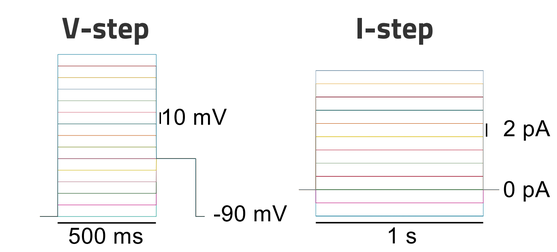

'Excitability' refers to the amplitude of overshoot between peak and steady-state voltage of action potential or rebound firing:

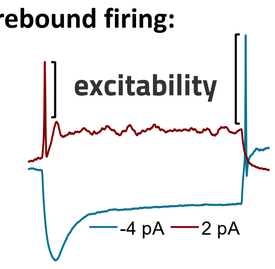

Figure 2. Firing behaviour and major current components differ between prototypical human and mouse SCLC lines.

For NCI-H889 and AF1165: A) Current density elicited by V-step protocol. B) Membrane potential during I-step protocols. C) Resting membrane potential (RMP), input resistance (IR), rebound excitability (RE), action potential (AP), and rheobase (RB) values. D) Early-activating potassium current calculated by subtraction of voltage steps from a -40 mV hold from those stepped from -90 mV.

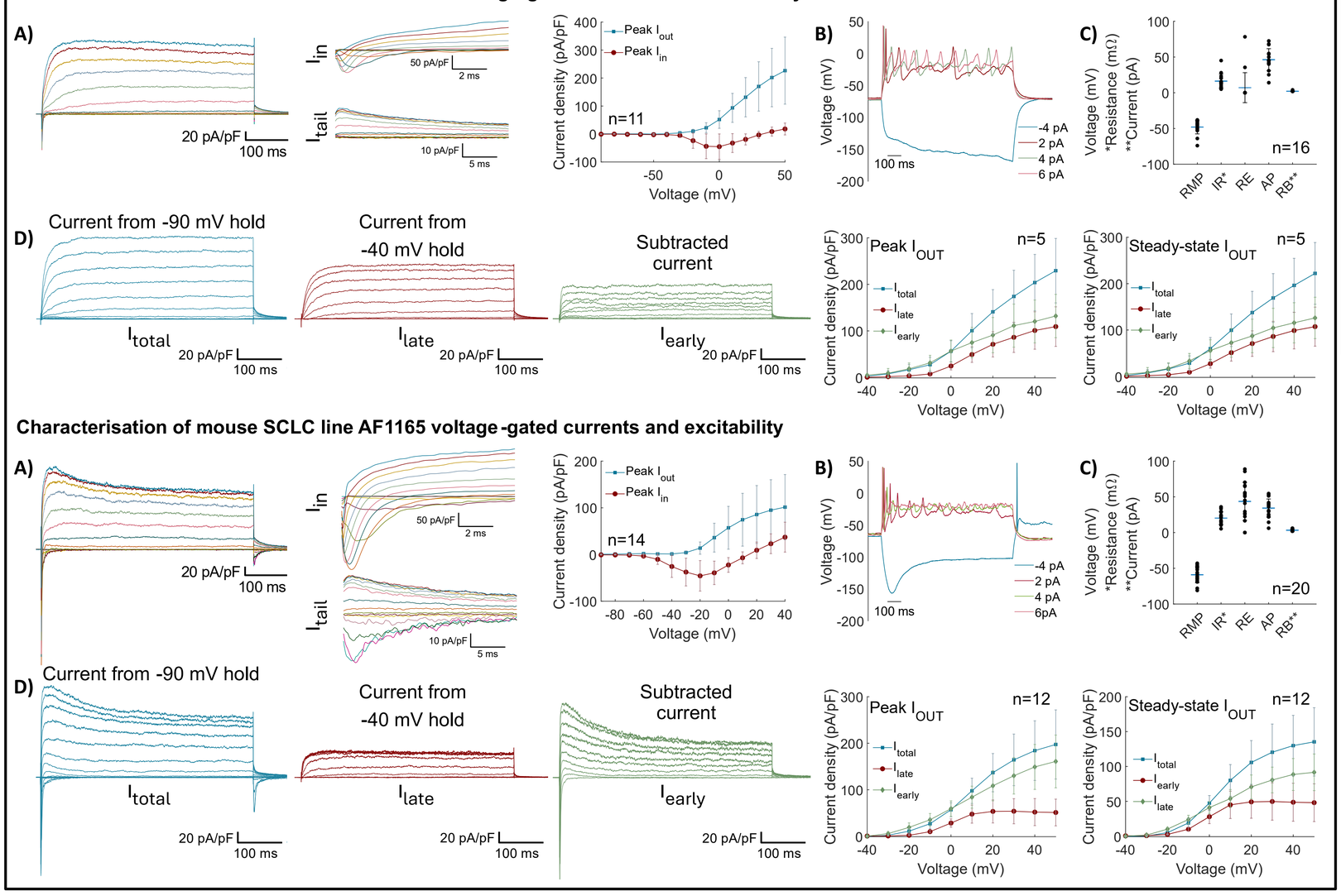

Figure 3. mSLCL line AF1165 displays both TTX-sensitive and TTX–resistant fast-inactivating inward current.

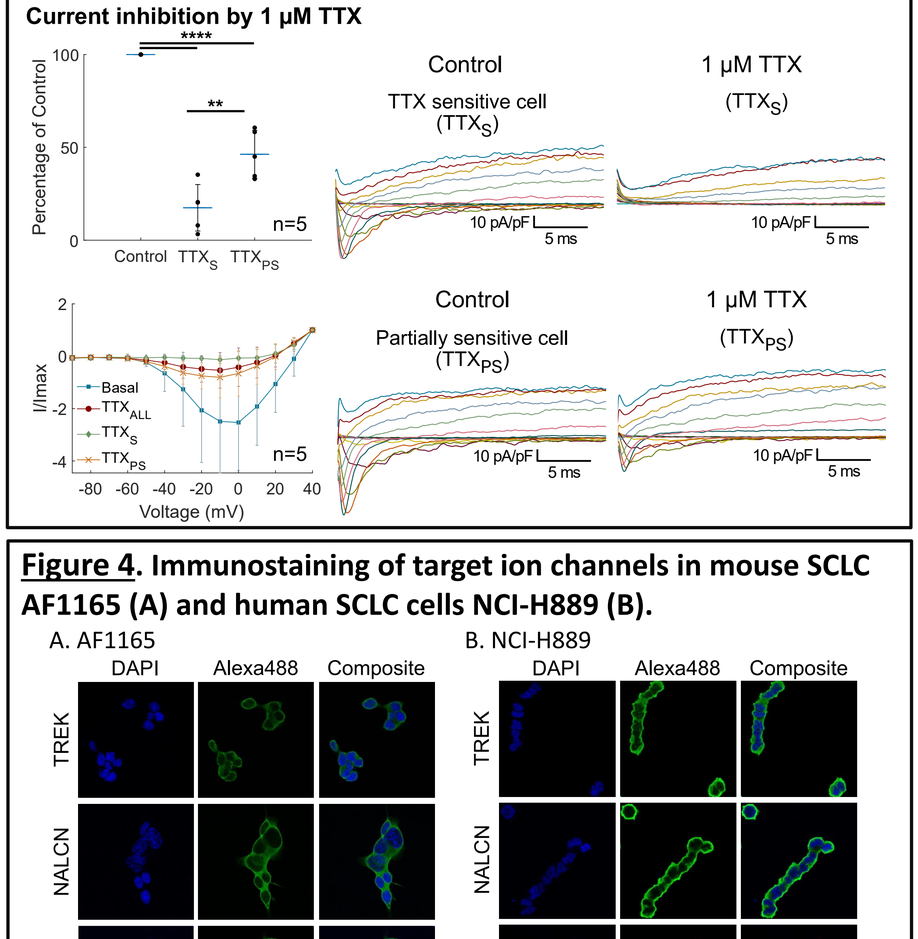

Figure 4. Immunostaining of target ion channels in mouse SCLC AF1165 (A) and human SCLC cells NCI-H889 (B).

Figure 5. TREK activator ML335 increases outward current and modulates firing in AF1165 SCLC cells. A) Application of 20 μM ML335[7] significantly increases outward current in whole-cell patch-clamp at + 40 mV step (n=7). B) Acute puff of 20 μM ML335 leads to hyperpolarization of the RMP. C) 20 μM ML335 modulates membrane characteristics of AF1165, leading to reduced excitability (n=6).

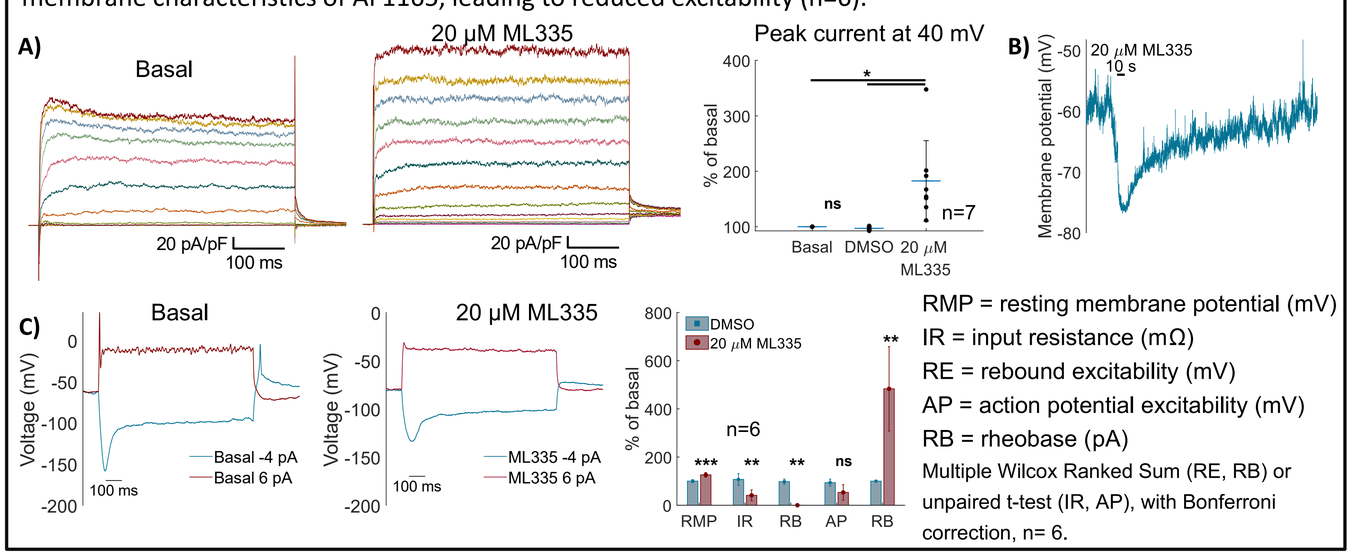

RMP = resting membrane potential (mV)
IR = input resistance (mΩ)
RE = rebound excitability (mV)
AP = action potential excitability (mV)
RB = rheobase (pA)

Multiple Wilcox Ranked Sum (RE, RB) or unpaired t-test (IR, AP), with Bonferroni correction, n= 6.

Figure 6. ATP produces both depolarisation and hyperpolarisation in AF1165, and can stimulate firing.

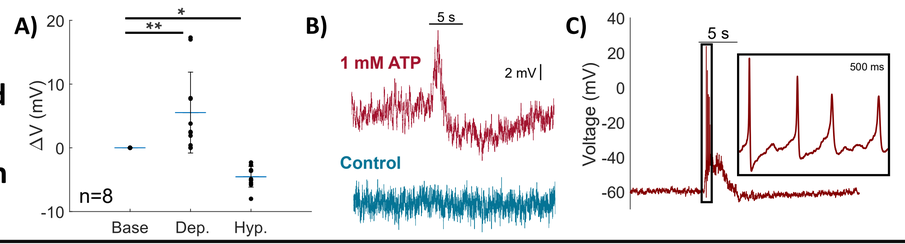

Figure 7. Evidence for functional expression of NALCN in AF1165 cells.

A) Isolation of a Na^+ 'leak' current using a K^+-free extracellular solution with 5 mM CsCl and CsCl intracellular solution (n=6).

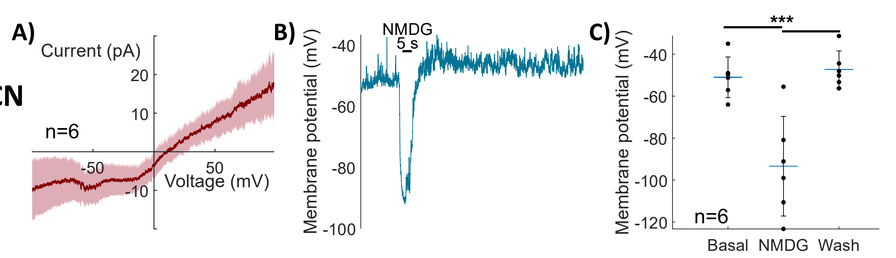

B) Acute application of NMDG, under the same conditions as (A), leads to significant hyperpolarisation of the RMP, suggesting the presence of an inward Na^+ current at rest that impacts the RM (one-way ANOVA with Tukey's correction, n=6).

Figure 8. Mathematical model simulates firing of AF1165 and impact of ion channel modulation.

A) Compartment model schematic of an excitable AF1165 SCLC cell. Key channels indicated in RNAseq data and functionally validated in AF1165 have been modelled, as well as a noise component. B) Simulated firing can be modulated by altering ion channel activity in the model.

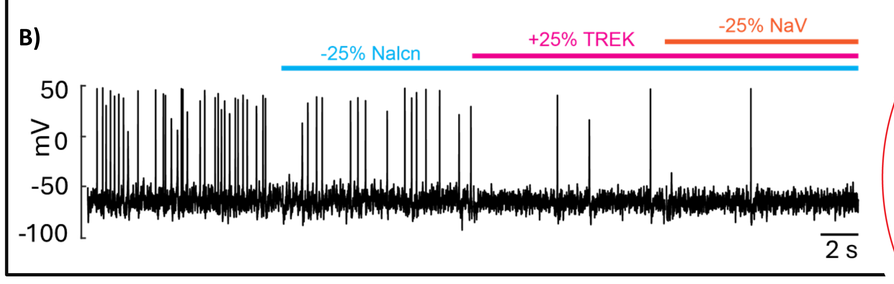

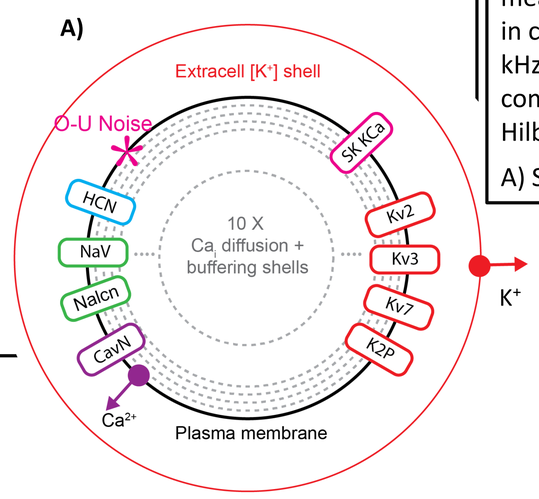

Figure 9. Depolarisation triggers capacitance transients indicative of vesicle fusion.

Capacitance changes measured by phase shift in current response to a 1 kHz sinusoidal voltage command, obtained by Hilbert transform[8].

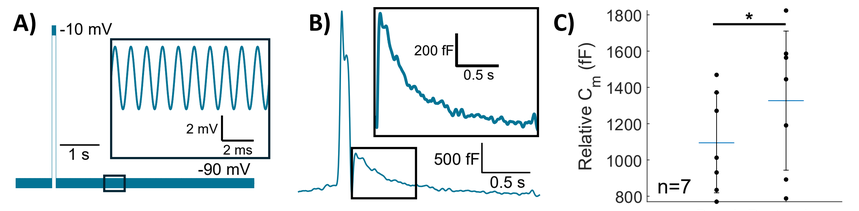

A) Stimulus. B) Relative capacitance response to depolarising pulse. C) Paired t-test (n=6).

CONCLUSIONS

- mSCLC line AF1165 and hSCLC line NCI-H889 both exhibit robust firing but display different current and firing characteristics.
- ICC staining and whole-cell patch-clamp electrophysiology suggest the functional presence of channels such as TREK-1, NALCN, and P2X and P2Y receptors in SCLC cells.
- A tuneable mathematical model simulates the firing behaviour of SCLC cells in response to ion channel modulation.
- Depolarisation of AF1165 can produce capacitance transients, suggesting vesicle fusion with the membrane and linking ion channel activity with secretion in SCLC cells.

Next steps: explore the impact of modulating excitability on proliferation and metastasis.

References: 1-Rudin, C.M. et al. (2021) 'Small-cell lung cancer', Nature Reviews. Disease Primers, 7(1), p. 3. Available at: doi.org/10.1038/s41572-020-00235-0. **2**-Peinado, P., Stazi, M., Ballabio, C. et al. Intrinsic electrical activity drives small-cell lung cancer progression. Nature (2025). //doi.org/10.1038/s41586-024-08575-7-. **3**-Takahashi, T. et al. (1989) 'p53: a frequent target for genetic abnormalities in lung cancer', Science (New York, N.Y.), 246(4929), pp. 491–494. Available at: /10.1126/science.2554494. **4**- Meuwissen, R. et al. (2003) 'Induction of small cell lung cancer by somatic inactivation of both Trp53 and Rb1 in a conditional mouse model', Cancer Cell, 4(3), pp. 181–189. Available at: doi.org/10.1016/s1535-6108(03)00220-4. **5**- Li, L. et al. (2019) 'Identification of DHODH as a therapeutic target in small cell lung cancer', Science Translational Medicine, 11(517), p. eaaw7852. Available at: doi.org/10.1126/scitranslmed.aaw7852. **6**- The MathWorks Inc. (2023). MATLAB version: 9.13.0 (R2023b), Natick, Massachusetts: The MathWorks Inc. https://www.mathworks.com. **7**- Lolicato, M. et al. (2017) 'K2P2.1 (TREK-1)-activator complexes reveal a cryptic selectivity filter binding site', Nature, 547(7663), pp. 364–368. Available at: doi.org/10.1038/nature22988. **8**- Bassetto, C.A.Z. et al. (2023) 'Ion channel thermodynamics studied with temperature jumps measured at the cell membrane', Biophysical Journal, 122(4), pp. 661–671. Available at: doi.org/10.1016/j.bpj.2023.01.015.

Supported by CRUK Multidisciplinary Project DRCMDP -Jun22\100016

CANCER RESEARCH UK

Engineering and Physical Sciences Research Council